Journal of Chromatography B 1144 (2020) 122078

Contents lists available at ScienceDirect

Journal of Chromatography B

journal homepage: www.elsevier.com/locate/jchromb

Zwitterionic HILIC tandem mass spectrometry with isotope dilution for rapid, sensitive and robust quantification of pyridine nucleotides in biological extracts

Lisa M. Røst[1], Armaghan Shafaei[1], Katsuya Fuchino, Per Bruheim*

Department of Biotechnology and Food Science, Faculty of Natural Sciences, NTNU Norwegian University of Science and Technology, NO-7481 Trondheim, Norway

ARTICLE INFO

Keywords:
Pyridine nucleotides
NAD(P)
Zwitterionic HILIC
Tandem mass spectrometry
^{13}C-isotope dilution

ABSTRACT

The pyridine nucleotides nicotineamide adenine dinucleotide (NAD) and nicotineamide adenine dinucleotide phosphate (NADP) are conserved coenzymes across all domains of life, and are involved in more than 200 different hydride transfer reactions supporting essential catabolic and anabolic functions. The intracellular levels of these metabolites, and the ratio of their oxidized to reduced forms regulate an extensive network of reactions ranging beyond metabolism. Hence, monitoring their intracellular levels provides information about, but not limited to, the metabolic state of a cell or tissue. Interconversion between oxidized and reduced forms, varying pH liability and varying intracellular concentrations of the different species leaves absolute quantification of the pyridine nucleotides analytically challenging. These polar metabolites are poorly retained on conventional reverseed-phase stationary phases without ion-pair reagents that contaminates the LC-system. Herein we demonstrate that zwitterionic HILIC-tandem mass spectroemtry can be applied to successfully resolve the pyridine nucleotides in biological extracts in a fast, robust and highly sensitive way. The presented method applies isotope dilution to compensate potential loss of these labile metabolites and is validated for low, medium and high biomass samples of two popular biological model systems; *Escherichia coli* and the human cell line JJN-3. High stability and rapid sample preparation without solvent removal allows for long sequence runs, making this method ideal for high-throughput analysis of biological extracts.

1. Introduction

The pyridine nucleotides nicotineamide adenine dinucleotide (NAD) and its phosphorylated analogue nicotineamide adenine dinucleotide phosphate (NADP) are conserved coenzymes across all domains of life. The oxidized forms NAD^+ and $NADP^+$ can undergo reversible reduction to form NADH and NADPH in an extensive network of hydride transfer reactions catalyzed by more than 200 different enzymes. Though structurally similar, both redox pairs have specialized metabolic functions. NAD^+ is reduced through central catabolic pathways such as glycolysis, the tricarboxylic acid cycle and β-oxidation of fatty acids, forming the link between these pathways and the respiratory chain. Inversely, NADPH is a cofactor in anabolic reactions such as reductive biosynthesis of fatty acids and cholesterol. In addition, both pyridine nucleotides have important regulatory roles. Hydrolysis of NAD^+ is linked to protein deacetylation by the sirtuin SIRT1 which targets proteins including a variety of metabolic enzymes, as reviewed in [1]. This leavies the NAD^+/NADH-ratio an important regulator of metabolic homeostasis. $NADP^+$ is an allosteric regulator of glucose 6-phosphate dehydrogenase (G6PD), catalyzing the first and committing step of the pentose phosphate pathway. Hence, increasing $NADP^+$-levels directs flux through this pathway on the expense of glycolysis in order to regenerate NADPH and sustain anabolic reactions. Roles outside strict metabolism is also described for both pyridine nucleotides. While NAD^+ is consumed in ADP-ribosylation, a post-translational modification implicated in cellular processes such as DNA repair, cell signaling and apoptosis (Reviewed in [2]), NADPH serves an important role in the cellular defense against reactive oxygen species by regenerating the antioxidant glutathione. Hence, absolute levels and ratios of oxidized and reduced NAD and NADP are crucial readouts of, but not limited to, the metabolic state of a cell. Absolute quantification is also a prerequisite for modeling and advanced biological interpretation involving enzyme kinetics. However, the physiochemical properties and high turnover of these metabolites makes them analytically challenging

* Corresponding author.
E-mail address: per.bruheim@ntnu.no (P. Bruheim).
[1] Lisa M. Røst and Armaghan Shafaei contributed equally to this work.

https://doi.org/10.1016/j.jchromb.2020.122078
Received 2 February 2020; Received in revised form 15 March 2020; Accepted 19 March 2020
Available online 21 March 2020

to quantify.

In the last decade, Liquid Chromatography Tandem Mass Spectrometry (LC-MS/MS) has become favored for analysis of nucleotide metabolites [3–8]. LC-MS/MS stands out for its high sensitivity and specificity, among other approaches such as high-performance liquid chromatography (HPLC) with UV detection [9–11], capillary electrophoresis [12,13], nuclear magnetic resonance (NMR) [14,15], and enzymatic approaches [16–18].

Pyridine nucleotides are highly polar, rendering them weakly retained and poorly resolved by conventional reversed-phase (RP) HPLC [19]. Consequently, approaches based on reversed-phase ion-pair mass spectrometry (IP-RP-HPLC-MS) [7,8], pentafluorophenylpropyl silica-based stationary phases (PFPP) [19], porous graphite stationary phases [20,21] and hydrophilic interaction liquid chromatography (HILIC) [4,6,22] have been developed for quantifying pyridine nucleotides in biological samples. In addition to poor retention, nucleotides are liable to fragment upon electrospray ionization (ESI), providing interfering isobaric species [4]. Further, redox pairs (i.e. NAD^+/NADH and $NADP^+$/NADPH) may present similar fragmentation profiles as they are only one mass unit apart. Therefore, sensitive, robust, and reliable chromatographic separation is required to avoid any false identification and inaccurate quantification of these metabolites [4,21]. HILIC offers effective separation of water-soluble metabolites that are not retained using conventional RP chromatography without the use of unfriendly buffers. However, many published reports favored IP-RP-HPLC-MS for analysis of pyridine nucleotides compared to HILIC-HPLC-MS, due to the better separation and peak shapes that ion-pair agents can provide, especially for phosphorylated metabolites [23,24]. Still, this approach has several drawbacks such as high background of the mobile phases, low MS signal intensity, and the requirement for dedicated instrumentation [19]. Bajad et al. (2006) tested four HILIC columns with three different stationary phases for separation of water-soluble metabolites, including an Atlantis – HILIC (silica) column with a negatively charged stationary phase, a Luna NH_2 (amino) column with a positively charged stationary phase, and Luna CN-cyano (hydrogen bond acceptor, not donor) and TSK Gel Amide 80-Amide (hydrogen bond acceptor and donor) columns with uncharged stationary phases. No peaks, or peaks of very poor shape were observed for phosphorylated pyridine nucleotides applying the cyano and silica stationary phases at acidic pH. In contract, peaks were observed for both amide at pH 6 and amino at pH 9, yet the peak shapes were generally better on the amino column [3]. The application of a HILIC amino column (Luna-NH_2) at pH 9.9 for the analysis of NAD^+ and other related nucleosides in yeast extracts was also reported by Evan et al. (2010) [6]. Zwitterionic sulfoalkylbetaine stationary phase has lately been employed for HILIC separations. In zwitterionic columns, the stationary phase carries permanent positive and negative charges at a ratio of 1:1, allowing electrochemical interactions to take place and increase rentention of polar analytes. Separation is thus accomplished by hydrophilic partitioning combined with weak ionic interactions [25]. Hence, zwitterionic HILIC might be an option for resolving pyridine nucleotides.

The two main concerns for quantifying the pyridine nucleotides NAD and NADP from biological samples are related to their stability and to the different endogenous concentration levels of these compounds. Further, an optimal extraction procedure is required to provide clean extracts low in interfering metabolites ensuring maximum recovery of targeted metabolites. Intracellular coenzymes are generally extracted using either hot or ice-cold organic solvents such as methanol, ethanol or acid/alkaline solutions [13,26,27]. However, organic-solvent extraction approaches have shown poor yields for polar adenosine nucleotides (NADP(H)) [7]. Further, the reduced and oxidized forms og pyridine nucleotides are stabilized at different pH ranges [7,8]. Oxidized pyridine nucleotides (NAD(P)) are more stable in acidic conditions and typically extracted from biological samples by standard acid-extraction protocols as discussed in [28]. However, the reduced pyridine nucleotides are more stable in alkaline conditions, and therefore extracted by alkaline-extraction protocols [27]. Hence, applying a proper extraction procedure balancing the requirements for both reduced and oxidized pyridine dinucleotides is crucial to allow for quantitative analysis of these highly polar metabolites.

Matrix effects will occur in every complex sample, especially when it contains complex biological matrices such as lysed cells. Matrix effects can dramatically influence the analytical performance in both qualitative and quantitative metabolite analysis, especially applying ESI-MS/MS. A well-described problem in ESI is the matrix effects caused by interfering compounds co-eluting with the metabolite of interest, leading to false negative or positive results [29]. Yet, robustness can be enhanced by isotope dilution (ID), i.e. the addition of isotopically labeled internal standards before extraction of metabolites. A great advantage of MS analysis is that it allows the use of isotopically labeled standard counterparts which can compensate matrix effects and loss or degradation of the target metabolites occuring during sample preparation and analysis [4].

In the present study, we developed and validated an LC-MS/MS method to identify and quantify the pyridine nucleotides NAD^+, NADH, $NADP^+$, NADPH and the flavin adenine dinucleotide FAD^+ in whole cell extracts from the cell line JJN-3 and *Escherichia. coli*. The method employs hot, alkaline extraction of cell pellets, sample preparation without solvent removal, ID, separation on a zwitterionic HILIC stationary phase, positive ESI and multiple reaction monitoring (MRM). We extensively investigated various extraction solvents, HILIC stationary phases and gradient profiles of the mobile phase system at varying pH and ammonium acetate buffer concentrations. The resulting method presented herein is rapid, robust and requires minimal sample preparation, allowing for analysis of large sample sets, making it applicable to a range of studies.

2. Material and methods

2.1. Analytical grade chemicals

LC-MS grade water and acetonitrile (ACN) were purchased from VWR. NAD^+ (N1511), NADH (N8129), $NADP^+$ (N5755), NADPH (N5130), FAD^+ (F6625), and LC-MS grade methanol (MeOH), ammonium acetate (73594), and ammonium hydroxide (5330030050) were purchased from Merck.

2.2. Cultivation and sampling

2.2.1. JJN-3 cells

The human plasma cell leukemia cell line JJN-3 (ACC 541, German Collection of Microorganisms and Cell Cultures) was cultured in RPMI-1640 medium (R8758, Merck) supplemented with 10% fetal bovine serum (F7524, Merck), 2 mM glutamine (K0283, VWR), 100 μg/ml gentamicin (G1272, Merck), and 2,5 μg/ml amphotericin (G1272, Merck). Cultures were maintained at 37 °C in a humidified atmosphere of 5% CO_2. Sampling was performed by pelleting 5×10^6, 1×10^7 and 1.5×10^7 cells (4 °C, 3 min, 150*g*) and rapidly quenching the pellet in LN_2. The pellets were stored at −80 °C until analysis.

2.2.2. Escherichia coli

E. coli K12 MG1655 (ATCC® 700926™) was cultured in mineral medium in baffled flasks at 37 °C with constant shaking at 200 rpm. Mineral medium was prepared in MilliQ-H_2O (MQ-H_2O) by dissolving 11.2 g/L Na_2HPO_4-$7H_2O$ (S9390, Merck), 3 g/L KH_2PO_4 (P5655, Merck), 0.5 g/L NaCl (27810.295, VWR), 0.5 g/L NH_4Cl (A9434, Merck), 0.2465 g/L $MgSO_4$-$7H_2O$ (M5921, Merck), 0.1470 g/L CaCl2-$2H_2O$ (223506, Merck) and 4 g/L glucose (101176 K, VWR), and 1mL/L of a trace element solution containing 10 g/L $FeSO_4$-$7H_2O$ (F8633,), 2.25 g/L $ZnSO_4$-$7H_2O$ (Z0251, k), 2 g/L $CaCl_2$-$2H_2O$ (223506), 1 g/L $CuSO_4$-$5H_2O$ (197722500), 0.38 g/L $MnCl_2$-$4H_2O$ (M5005), 0.14 g/L H_2BO_3 (B6768) and 0.1 g/L $(NH_4)_6Mo_7O_{24}$-$4H_2O$ (1011820250), all

from Merck. Exponentially growing cultures were sampled at OD_{600} 1–1.25 by pelleting 2, 5 and 10 ml of cell suspension (4 °C, 5 min, 4500*g*) and rapidly quenching the pellet in LN_2. The pellets were stored at −80 °C until analysis.

2.2.3. Preparation of $U^{13}C$- isotopologues of target metabolites from E. coli

E. coli K12 MG1655 was cultured as described with $^{13}C_6$-glucose (> 99%, 389374, Merck) substituting naturally labeled glucose in the medium. Cultures were sampled at OD_{600} 3–3.5 by pelleting 10 ml of cell suspension as described.

2.3. Extraction of intracellular metabolites

Intracellular metabolites were extracted from pellets thawed on ice in 0.3 ml warm (80 °C) ACN:MeOH:water (60:20:20 v/v) with 15 mM ammonium acetate pH 9.7, added 10% of a ^{13}C-labeled *E. coli* extract for ID. Warm extraction was performed at constant shaking (80 °C, 800 rpm) for 3 min, before extracts were cleared of cell debris and large molecules in two consecutive centrifugation steps at 4 °C; 2 min at 4500*g*, and 5 min at 14,000*g* in 3-kDa-molecular-weight spin cut-off filters (516–0228, VWR).

2.4. Instrumentation conditions

2.4.1. LC

Chromatographic separation was performed on a Waters AQUITY I-Class UPLC equipped with an online vacuum degasser, a binary pump, an autosampler, and a thermostated column compartment. HILIC was carried out on an AdvanceBio MS Spent Media 2.1 × 100 mm column (Agilent, 675775-901) with a particle size of 2.7 µm, with mobile phases (A) water:ACN (50:50 v/v) and (B) water:ACN (20:80 v/v), both with 15 mM ammonium acetate adjusted to pH 9.7 with ammonium hydroxide. Following initial mobile phase conditions of 10% A, A was increased to 65% over 9 min and then reduced to 10% over 0.5 min, before the column was re-equilibrated for 4.5 min. The flow rate was 0.2 ml/min, the column temperature was maintained at 30 °C, the injection volume was 2 µL, and the temperature of the autosampler was set to 6 °C.

2.4.2. MS/MS

Tandem mass spectrometry (MS/MS) was performed on a Waters Xevo TQ-XS triple quadrupole mass spectrometer system equipped with an ESI source operated in positive mode. The spectra were acquired in multiple reactions monitoring (MRM) mode. The number of data points for each SRM transition was 12. Dwell time ranged from 28 to 38 ms for all metabolites. Instrument control was performed from MassLynx 4.2 and data acquisition was performed in TargetLynx application manager of MassLynx 4.2 (Waters). Argon gas was chosen as collision gas, nitrogen was chosen as nebulizer gas and heater gas. The MS conditions were optimized as follows: capillary voltage 2.5 kV; cone voltage 20 V; source offset voltage 30 V; source temperature 150 °C; desolvation temperature 400 °C; cone gas flow 150 L/h; desolvation gas flow 800 L/h; collision gas flow 0.15 ml/min; nebulizer gas flow 6 Bar. For optimization of MS parameters, the standard metabolites were prepared at a concentration of 10 µM in ACN:Water (80:20 v/v) and individually introduced into the (+)-ESI source by direct infusion at a flow rate of 10 µL/min. Optimal MRM parameters including precursor ion, product ions transitions, and collisions energies obtained for each standard are presented in Table 1. The product ions of corresponding $U^{13}C$-isotopologues were obtained by daughter ion scans from $U^{13}C$-precursors from $U^{13}C$-labeld *E. coli* extracts, applying the optimized MS conditions and a scan speed of 5000 amu/second.

Table 1
Optimized MRM parameters for target flavin/pyridine nuceotides and corresponding $U^{13}C$-isotopologues applied for isotope dilution.

Compound	Retention window (min)	Precursor ion (*m/z*)	Product ion (*m/z*)	Collision (V)
NAD^+	5.9–6.9	664.1	428*	26
			524	18
NADH	4.9–5.9	666.1	514.1	26
			649*	17
$NADP^+$	8.3–9.3	744.1	508	30
			604*	20
NADPH	7.5–8.5	746.1	301	32
			729*	17
FAD^+	4.1–5.1	786.1	348*	22
			439.1	28
$U^{13}C$-NAD^+	5.9–6.9	685.1	438*	26
			539	18
$U^{13}C$-NADH	4.9–5.9	687.1	528.1	26
			670*	17
$U^{13}C$-$NADP^+$	8.3–9.3	765.1	518	30
			619*	20
$U^{13}C$-NADPH	7.5–8.5	767.1	313	32
			750*	17
$U^{13}C$-FAD^+	4.1–5.1	813.1	358*	22
			465.1	28

* Quantifier ion.

2.5. Optimization of method parameters

2.5.1. Stationary phase

An AQUITY BEH Amide 2.1 × 100 mm column (186004801, Waters) fitted with an ACQUITY BEH Amide VanGuard 2.1 × 5 mm pre-column (186004799, Waters), both with a particle size of 1.7 µm, a SeQuant ZIC-pHILIC 2.1 × 100 mm column (1.50462, Merck) with a particle size of 5 µm, and an AdvanceBio MS Spent Media 2.1 × 100 mm column (Agilent, 675775–901) were tested for separation of the target metabolites.

2.5.2. Ionization mode

E. coli extract and analytical standards in pure extraction solvent background were analyzed as described in Sections 2.4.1 and 2.4.2. Two different ion sources were tested; an ESI (Waters) and an UniSpray (US, Waters) source, both operating in positive mode. The US source was tuned with Leucine Encephalin (67 pg/µL) at an impactor voltage of 2 kV. Samples were run as described for ESI, with the impactor voltage optimized to 0.5 kV. The signal to noise ratio (S/N) of target metabolites from both background matrices and ion sources were recorded.

2.6. Extraction solvent

Parallel pellets of JJN-3 and *E. coli* were extracted as described in Section 2.3 applying four different extraction solvents: 1) ACN:water (80:20 v/v, 15 mM ammonium acetate, pH 9.7), 2) ACN:water (80:20 v/v, 5 mM ammonium acetate, pH 9.7), 3) ACN:water (80:20 v/v, pH 9.7 adjusted with ammonium hydroxide), and 4) ACN:MeOH:water (60:20:20 v/v, 15 mM ammonium acetate, pH 9.7). Recoveries of the target metabolites were expressed as the ratio of the response (peak area ratio of the analyte to corresponding ^{13}C isotopologue) to the first injection. The samples were analyzed in triplicates to assign the percentage recovery.

2.7. Preparation of calibration standards

Single stock solutions (2 mM) of the target metabolites were prepared in water on the day of analysis. Calibration standard mixes containing all target metabolites were prepared in the extraction solvent (described in Section 2.3) and *E. coli* and JJN-3 matrices (extracted

as described in Section 2.3), all supplemented with 10% ^{13}C-labeled *E. coli* extract. Serial dilutions of the stock standard solutions were used to generate calibration standards in the range of 156.25–20,000 nM.

2.8. Method validation

The method was validated in accordance to U.S. Pharmacopeia [30] and advises for application in bioanalytical method validation [25,31].

2.8.1. Linearity and sensitivity

Linearity of the method was evaluated by injecting a 13-point dilution series of calibration standards in both extraction solvent and biological matrices to calculate calibration curves for each target metabolite by linear regression. To estimate the method sensitivity, the limit of detection (LOD) and limit of quantification (LOQ) were calculated from the S/N of serial dilutions of a calibration standard mix prepared in the concentration range of 100–0.78 nM. The LOD and LOQ are expressed as the concentration with corresponding S/N equal to 3 and 10 in the calibration standards, respectively.

2.8.2. Precision and accuracy

The precision and accuracy of the method was evaluated by intra-day and inter-day analyses of quality control standards (QCs) prepared at three different concentrations; low (LQC; 312.5 nM), medium (MQC; 2500 nM) and high (HQC; 7500 nM). QCs were injected six times per day and for six consecutive days for intra-day and inter-day analysis, respectively. The resulting corrected responses of the replicate analysis were used to calculate the coefficient of variance (CV %) and hence precision. In addition, the % CV was calculated for 6 injections of low, medium and high biomass prepared from JJN-3 (5, 10, 15 $\times$ 10^6 cells) and *E. coli* (2, 5 and 10 ml cell suspension at OD_{600nm} 1.25). The % bias was calculated as mean concentration relative to nominal concentration to express accuracy (% bias or trueness) of the method.

2.8.3. Recovery and matrix effects

To evaluate if ID could be applied to compensate potential loss of sample and random errors in a long sequence run, one JJN-3 and one *E. coli* extract were injected once an hour for 12 hours and quantified with and without correction. To evaluate potential matrix effects, the slopes of calibration curves prepared in extraction solvent was compared to the slopes of calibration curves prepared by standard addition to whole cell extracts of JJN-3 and *E. coli*. Due to unavailability of neat cell extracts (without the target metabolites), the calibration curve in extraction solvent was prepared in a background of target metabolites. The concentration of target metabolites in the background mix was selected to mimic the baseline concentration of target metabolites in biological extracts. The extent of matrix ion suppression/enhancement effect ($ME_{ionization}$) was calculated according to the following equation:

$$ME_{ionization} = \frac{S_{slope\ of\ \ target\ metabolite\ \ in\ \ matrix} - S_{slope\ of\ \ target\ metabolite\ in\ extraction\ solvent}}{S_{slope\ of\ target\ metabolite\ in\ extraction\ solvent}} \times 100 \quad (100)$$

In addition, the target metabolite concentrations in three JJN-3 and *E. coli* whole cell extracts were quantified by interpolation from both the extraction solvent and corresponding biological matrix calibration curves to calculate the percentage of agreement. The relative recovery of the target metabolites was determined by spiking 10 µL of QC samples to 90 µL of pooled JJN-3 or *E. coli* whole cell extracts prepared as described in Section 2.3, to a final spiked concentrations of 312.5 nM (LQC), 2500 nM (MQC) and 7500 nM (HQC). The baseline (unspiked) and spiked samples were analyzed and the % recovery was assigned by comparing the nominal concentration (baseline concentration + spiked concentration) to the corresponding measured concentration.

2.8.4. Stability

The stability of quality control samples (LQC, MQC and HQC) of analytical standards and of JJN-3 and *E. coli* extracts, all prepared as described in Section 2.8.2, were evaluated under three different conditions; storage in the auto sampler (6 °C) for 24 h, storage at room temperature for 24 h, and after one, two, and three repeated freeze-thaw cycles.

2.9. Application

Extract concentrations of target metabolites were measured to determine absolute intracellular concentrations in JJN-3 and *E. coli*. The measured concentration was corrected for concentration during sample preparation and normalized to cell density (5 $\times$ 10^5 cells/mL) or cell dry weight (DW, 0.43 g/L) of the extracted JJN-3 and *E. coli* samples, respectively. Intracellular concentrations were calculated from the experimental cell volume (1.1 pL) of a JJN-3 cell and the specific cell volume (3.33 $\times$ 10^{-3} L/g) of *E. coli,* the latter calculated from the volume (1 $\times$ 10^{-15} L) and DW (3 $\times$ 10^{-13} g) of an *E. coli* cell, as listed in the *E. coli* metabolome database (ECMDB) [32].

3. Results and discussion

3.1. Analytical method development

As HILIC was considered a promising strategy for retaining pyridine nucleotides without the use of contaminating ion-pair reagents, three different HILIC stationary phases were tested for the separation of target metabolites; BEH Amide and two zwitterionic stationary phases, ZIC-pHILIC and AdvanceBio MS Spent Media. All stationary phases were tested with mobile phases (A) ACN:water (50:50, v/v) and (B) ACN:water (80:20, v/v), 5–10 mM ammonium acetate, pH 9.0. The target metabolites were close to baseline resolved on both BEH Amide and ZIC-pHILIC stationary phases. However, split peaks were observed for NADH and NADPH, while $NADP^+$ was severely tailing (Fig. 1A and B). The peak shape improved significantly applying the AdvanceBio stationary phase (Fig. 1C). In the BEH Amide column, ethylene bridged hybrid particles are bonded to a trifunctional amide phase. This particular stationary phase is uncharged, yet demonstrating high polarity and hydrogen bonding properties [33], but no ionic interactions with highly charged metabolites. Thus, incomplete interaction of stationary phase with the charged target metabolites might explain the poor peak shapes observed for this column. The retention mechanism in zwitterionic HILIC is complex and not governed by one single process. Two mechanisms simultaneously taking place might explain the complex retention: 1) partitioning of polar analyte between the mobile phase and stationary phase, and 2) adsorption of polar analyte at the ionic sites of the stationary phase due to electrostatic interactions (ion-ion and dipole-ion interactions) [34]. In the two zwitterionic columns tested for separation of pyridine nucleotides, sulfoalkylbetaine functional groups are bonded to polymer support (ZIC-pHILIC) or silica gel support (AdvanceBio). Zwitterionic stationary phases carry permanent positive and negative charges at a ratio of 1:1 [25,33]. However, because of the spatial orientation of the sulfonic group at the distal end of the zwitterionic moiety in silica bonded zwitterionic HILIC, this stationary phase carries a slight negative surface charge [35]. This may cause weak electrostatistic interactions between the stationary phase with silica gel support and the target metabolites. These interactions may be weaker or not occurring between the target metabolites and the stationary phase with polymer support, which could explain the better peak shape of silica based zwitterionic HILIC compared to the polymer based ZIC-pHILIC (Fig. 1B and Fig. 1C). The better peak shapes left the AdvanceBio column the best candidate for further optimization of separation conditions. Mobile phases were prepared with 5, 10, and 15 mM ammonium acetate in a pH-range from 9.4 to 9.9. Various buffer and pH combinations were trailed with a number of gradient profiles to determine optimal separation conditions. A mobile phase system buffered with 15 mM ammonium acetate at pH 9.7 did yield superior separation and peak shape in both calibration standards and all tested

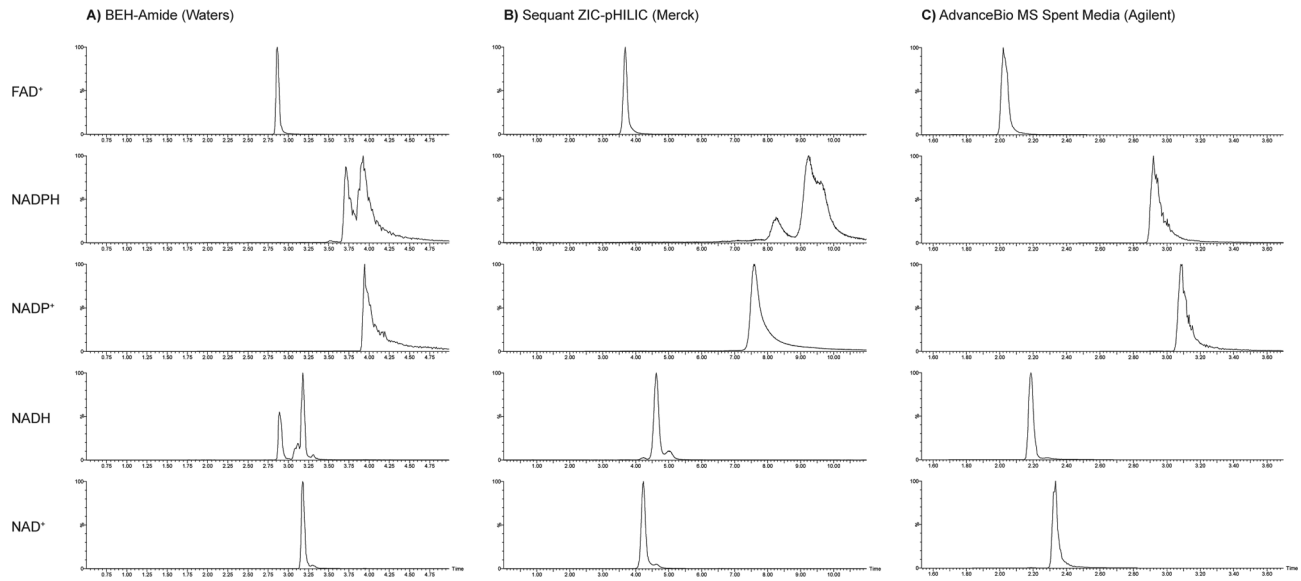

Fig. 1. Total ion chromatograms of a 20 uM mix of FAD^+, NADPH, $NADP^+$, NADH and NAD^+ analytical grade standards, as separated on a (A) BEH-Amide stationary phase (Waters), a (B) SeQuant ZIC-pHILIC stationary phase (Merck) and a (C) AdvanceBio MS Spent Media stationary phase (Agilent). The standards were separated with a linear gradient of (A) ACN : water (50:50, v/v) and (B) ACN water:(80:20, v/v), both with 5–10 mM ammonium acetate, pH 9.0, after being dissolved in (B).

biological extracts (Fig. 2). The effect of high buffer concentration on peak shape is also reported by Zborníkováa et al. for zwitterionic columns [25]. The retention times of this system were consistent throughout each sequence run, but minor shifts were sometimes observed between runs, e.g. after preparing fresh mobile phases or installing a new column. Yet, the peak shape and between-compound retention times were allways consistent.

Lastly, optimization of ionization conditions was performed to attain the highest possible sensitivity. After establishing higher sensitivity in positive compared to negative mode, positive ionization was tested with two ion sources, ESI and UniSpray (US). US is an impact ionization source, in which formation of ions is directed by a heated nebulized spray of liquid onto a surface with an applied voltage [36]. In contrast, in ESI formation of ions is directed by a heated high velocity spray from a charged capillary. Improved sensitivity in US compared to ESI has been reported [37], however, this strongly depends on the chemical properties of the target compound and the chromatographic mode [38]. Extracts of *E. coli* and calibration standards were analyzed using both ion sources, yielding a higher S/N in ESI compared to US for all target metabolites (Table S1). This effect was more pronounced in biological samples than calibration standards, especially for $NADP^+$ and NAPDH ($\geq$5-fold). Thus, ESI was chosen for further method validation and application.

3.2. Preparation of whole cell extracts

An extraction procedure for pyridine dinucleotides from quenched cell pellets was developed and optimized for two commonly applied biological systems, namely *E. coli* and a human suspension cell line, JJN-3. Loss and interconversion of these target metabolites has been reported for several methods of solvent removal [39,40]. As such, the extraction method and panel of candidate extraction solvents (Table 2) were chosen to balance the need to stabilize and concentrate the labile target metabolites with the need for compatible HILIC solvents. Low pH is negatively affecting the stability of the labile reduced nicotineamide adenine dinucleotides [27], thus all extraction solvents were buffered at high pH, and acidic extraction was not investigated. Rather, high standard recovery has been reported for $NADP^+$ and NADPH in hot (95–100 °C) water at high pH [40] and for all four NAD(P)-metabolites in boiling ethanol [6,8], indicating that a rapid hot extraction step is tolerated. Lastly, ACN is commonly applied to precipitate protein and thus quench residual enzymatic activity, which may else cause unwanted interconversion or consumption of target metabolites. Thus, pellets were reconstituted in $\geq$ 3 $\times$ packed cell volume (PCV) of an extraction solvent system of ACN and water at high pH and extracted at continuous shaking at 80 °C for 3 min. As direct injections of supernatants from biological extracts were found to cause increased LC-system pressure over time, extracts were cleared in yet another step; by spin filtration with 3 kDa cutoff. Four ACN : water solvent systems were considered for extraction. Solvent 1; mobile phase B applied for chromatographic separation (ACN: water 80:20 with 15 mM ammonium acetate, pH 9.7) worked well for both low biomass samples and spiked analytical standards, yielding reproducible responses and perfectly linear calibration curves (Data not shown). However, this was not reproduced in medium biomass samples, as demonstrated by their % recoveries ranging from 15 to 60% over four repeated injections (Solvent 1, Table 2), which is well below the acceptance criteria of $\geq$70%. The cause of this was found to be phase-separation of extracts possibly triggered by the high salt content of biological samples. Decreasing the concentration of, or even eliminating ammonium acetate from the extraction solvent (Solvent 2 and 3, respectively) did not improve recovery (Table 2) nor prevent phase separation. Thus, the salt content of the biological samples itself likely forced phase separation in an 80:20 ACN:water solvent system. Though the low miscibility severely affected recovery, it had no observable effect on chromatographic peak shape of the target metabolites. This phenomenon was circumvented by introducing 20% MeOH to the extraction solvent system, as demonstrated by the excellent recovery of a 60:20:20 ACN:MeOH:water solvent system (Solvent 4, Table 2). This system is actually a low-MeOH version of the extraction solvent successfully applied by Lu and colleagues [38] for cold extraction of nicotineamide adenine dinucleotides from human cell pellets. However, increasing the MeOH content of the extraction solvent above 20% on the expense of ACN was detrimental to chromatographic peak shape and was not tested further. To circumvent potential volume changes due to MeOH evaporation, extraction was performed in closed tubes which were cooled before the extracts were transferred.

3.3. Method validation

3.3.1. Linearity and sensitivity

A 13-point calibration curve was constructed for each target metabolite by plotting concentration versus corrected response (peak area to

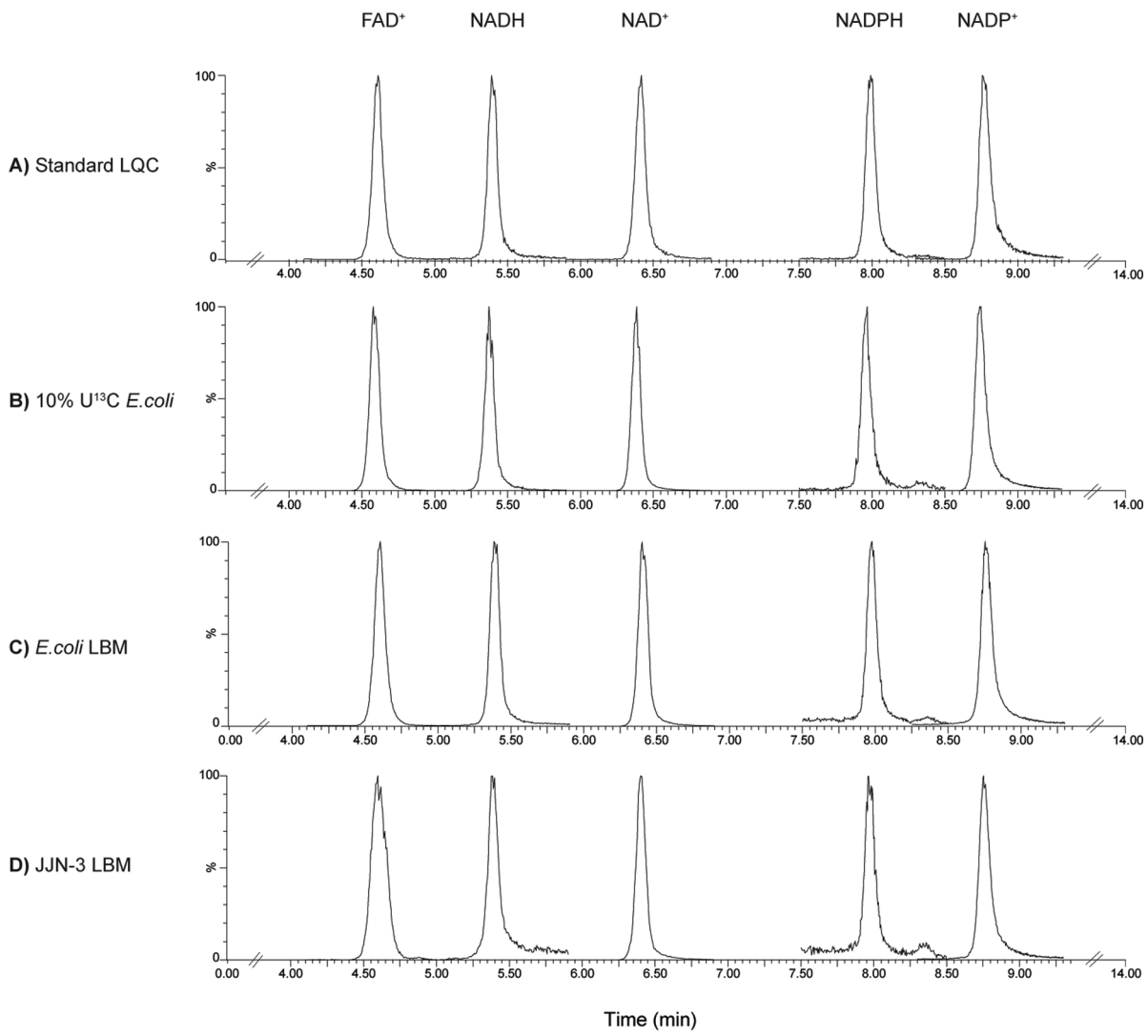

Fig. 2. Overlaid total ion chromatograms of FAD^+, NADH, NAD^+, NADPH and $NADP^+$ from (A) a low quality control (LQC, 312.5 nM) analytical standard mix, (B) a 10% $U^{13}C$ *E. coli* whole cell extract as applied for isotope dilution (C) a low biomass (LBM) *E. coli* whole cell extract and (D) a LBM JJN-3 whole cell extract. The total run time of the method is indicated by the broken axes. All samples were extracted/dissolved in ACN:MeOH:water (60:20:20 v/v) with 15 mM ammonium acetate pH 9.7, and separated with a linear gradient of (A) ACN:water (50:50, v/v) and (B) ACN:water (80:20, v/v) with 15 mM ammonium acetate, pH 9.7.

peak area of corresponding ^{13}C-isotopologue). The slope, intercept and correlation coefficient from linear regression was assessed and applied to interpolate the extract concentrations. In addition, standard addition to whole cell extracts of JJN-3 and *E. coli* was performed to evaluate potential matrix effects that may alter the ionization efficacy and implement bias. Close to perfect linearity ($R^2 > 0.985$) was observed in the range of 156.15–10,000 nM for all calibration curves, both when prepared in extraction solvent and by standard addition to biological extracts. The sensitivity of the method was evaluated by determining the LOD and LOQ. The LOD is defined as the lowest detectable concentration of analyte that an analytical system can reliably differentiate from the background level (S/N = 3). The LOQ is the lowest

Table 2
Recovery of target flavin/pyridine nucleotides extracted from high biomass *E. coli* pellets (5 ml, OD 3) listed for four tested extraction solvents. CV: coefficient of variation.

Compound	Solvent 1		Solvent 2		Solvent 3		Solvent 4	
	Recovery (%)	% CV	Recovery (%)	% CV	Recovery (%)	% CV	Recovery (%)	% CV
NAD	28.3–65.6	42.1	14.2–60.1	72.8	25.2–55.7	36.5	98.0–101.0	1.5
NADH	29.4–71.6	43.6	10.6–60.2	84.7	14.7–46.6	55.2	98.4–102.4	2.1
NADP	15.7–56.3	63.4	4.7–50.7	116.4	12.6–44.9	61.0	98.2–101.6	1.8
NADPH	14.6–60.7	69.5	3.9–48.7	119.1	9.4–40.7	70.8	98.1–102.6	2.3
FAD	20.0–51.4	50.4	7.0–44.4	100.2	16.5–39.7	44.8	96.9–103.4	3.3

Solvent 1: ACN: water (80:20, 15 mM ammonium acetate, pH 9.7).
Solvent 2: ACN: water (80:20, 5 mM ammonium acetate, pH 9.7).
Solvent 3: ACN: water (80:20, adjusted pH to 9.7 with ammonium hydroxide).
Solvent 4: ACN: MeOH : water (60: 20: 20, 15 mM ammonium acetate, pH 9.7).

Table 3
Limit of detection (LOD), limit of quantification (LOQ), intra-day and inter-day precision and accuracy of the optimized LC-MS/MS method. CV: coefficient of variation, L/M/HBM: low/medium/high biomass, L/M/HQC: low/medium/high quality control.

Compound	LOD (nM)	LOQ (nM)	Intra-day precision (% CV, n = 6)			Intra-day accuracy (% bias, n = 6)			Inter-day precision (% CV, n = 6)			Inter-day accuracy (% bias, n = 6)			Intra-day precision in JJN-3 (% CV, n = 6)			Intra-day precision in *E. coli* (% CV, n = 6)		
			LQC	MQC	HQC	LQC	MQC	HQC	LQC	MQC	HQC	LQC	MQC	HQC	LBM	MBM	HBM	LBM	MBM	HBM
NAD	0.8	3	2.0	3.0	3.9	12.6	17.7	12.6	6.3	3.8	2.2	20.8	18.3	13.7	3.4	3.3	1.2	1.7	2.1	1.1
NADH	6	12	1.7	2.9	4.0	0.3	1.3	0.4	6.2	7.1	10.9	3.7	−4.5	−17.0	3.1	3.9	5.9	6.8	8.6	4.5
NADP	0.8	3	4.2	3.8	4.1	15.8	5.9	3.2	4.3	2.7	4.2	17.8	2.0	−2.9	3.6	4.2	4.4	2.7	4.0	4.3
NADPH	3	12	5.3	1.4	1.9	7.1	2.2	1.2	3.4	3.1	7.0	7.1	−2.7	−10.2	6.2	4.3	3.7	7.8	9.0	4.9
FAD	0.8	3	2.3	1.7	4.4	2.4	0.9	−1.4	1.6	6.6	3.5	4.4	−5.5	−3.2	2.7	4.1	7.3	3.5	3.0	2.9

quantifiable level of analyte that can be measured with a standard level of confidence, and is typically calculated using a S/N = 10. The LODs and LOQs for all targeted metabolites were in the range of 0.78–6 nM and 3–12 nM, respectively (Table 3), which is far below the concentration in all tested whole cell extract. Thus, the method is sensitive enough for quantification of pyridine dinucleotides in whole cell extracts from JJN-3 and *E. coli*, and ≥ 9 times more sensitive than the IP-RP-MS/MS method reported by Seifar et al. [8].

3.3.2. Precision and accuracy

Intra-day and inter-day variation was determined for three QCs (LQC, MQC and HQC) relevant to the average level of pyridine nucleotides measured in whole cell extracts of *E. coli and JJN-3* cells by performing six replicate injections in one single day (intra-day), and one replicate injection for six consecutive days (inter-day). Intra-day variation was also determined for three whole cell extracts of *E. coli and JJN-3* sampled at low, medium and high biomass (LBM, MBM, and HBM). The % coefficient of variation (CV) was calculated to evaluate the precision of the method and estimate repeatability and intermediate precision of the assay. The % CV ranged from 1.1 to 10.9% for both intra-day and inter-day injections. This complies with the acceptable limit of maximum 20% deviation from the mean value. This confirmed that the method is precise, repeatable and applicable for use over days during routine analysis. The bias ranged from −17.0 to 20.8% for both intra-day and inter-day studies. Hence, the obtained results were in agreement with the acceptance criterion for method accuracy (≤20%) (Table 3).

3.3.3. Recovery and evaluation of matrix effects

In this study, ID was applied to compensate loss or enhancement of target metabolites upon extraction and analysis. As no isotopically labeled or deuterated standards were commercially available, an $U^{13}C$-labeled extract was prepared from *E. coli*. *E. coli* was cultured for five passages in mineral medium with $U^{13}C$-glucose as the sole carbon

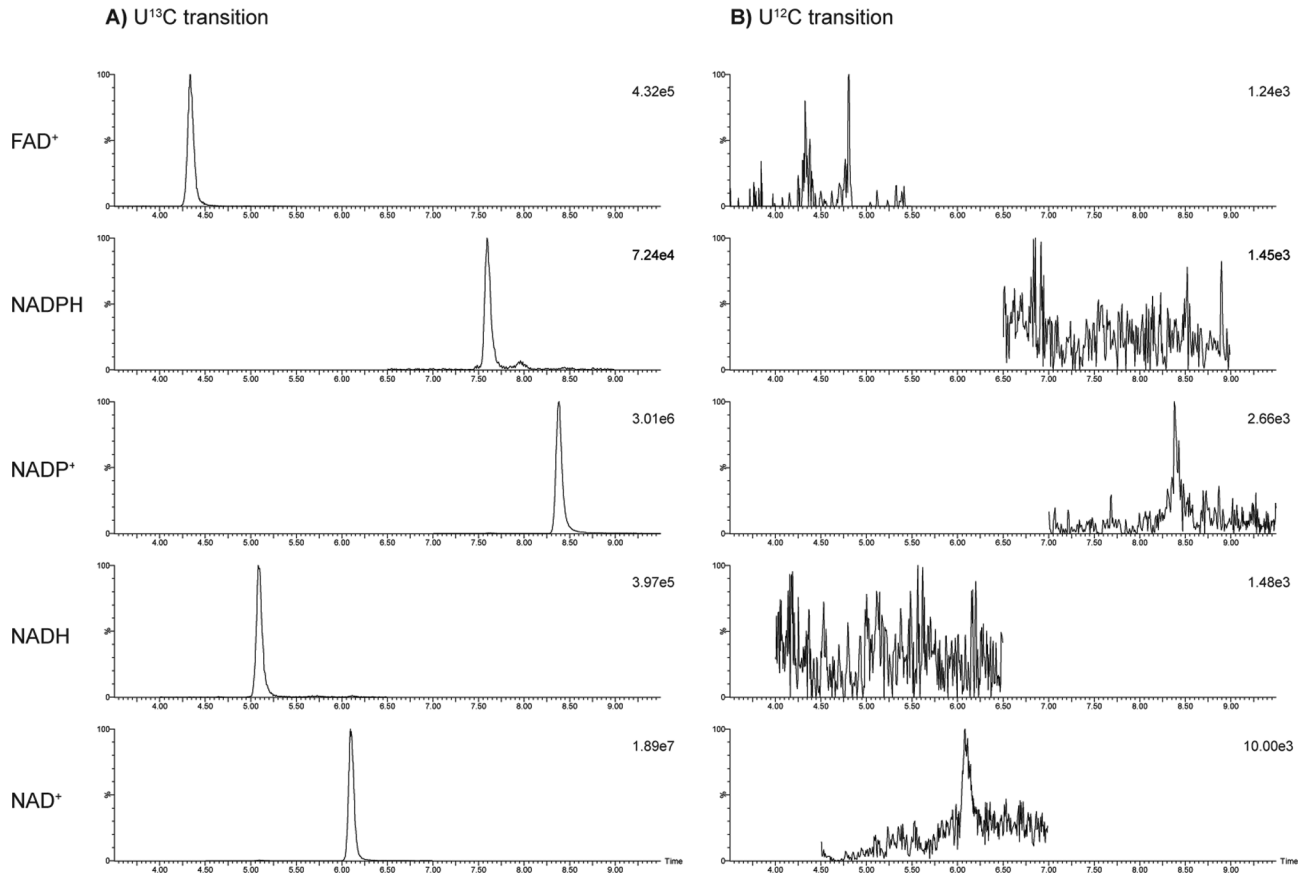

Fig. 3. Total ion chromatograms of a 10% $U^{13}C$ *E. coli* whole cell extract as applied for isotope dilution, (A) $U^{13}C$-transitions and (B) $U^{12}C$-transitions with relative response listed. Extraction was performed in ACN:MeOH:water (60:20:20 v/v) with 15 mM ammonium acetate pH 9.7, and extracts were separated with a linear gradient of (A) ACN:water (50:50, v/v) and (B) ACN:water (80:20, v/v) with 15 mM ammonium acetate pH, 9.7.

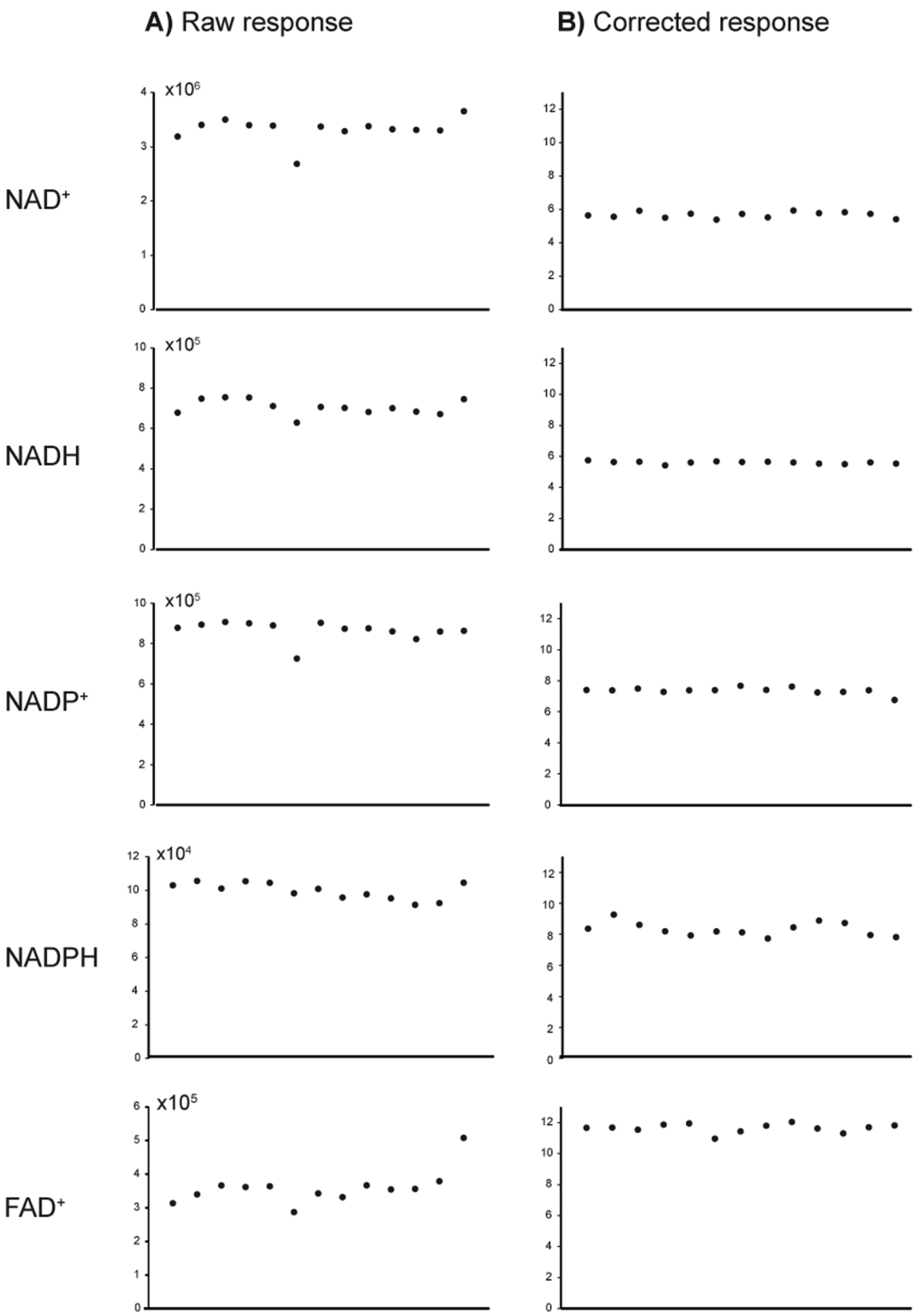

Fig. 4. Response of flavin/pyridine nucleotides in an *E. coli* whole cell extract injected hourly for 12 hours, presented (A) without (raw response), and (B) with isotope dilution.

Table 4
Recovery of target metabolites and recorded matrix effect for the optimized extraction protocol and LC-MS/MS method.

Compound	*Matrix effect (%)		*E. coli*		JJN-3		*E. coli*			JJN-3			
	E. coli	JJN-3	Spiked concentration (nM)	Relative recovery (%)	Spiked concentration (nM)	Relative recovery (%)	Sample	Concentrations (nM)		Percentage agreement (%)	Sample	Concentration (nM)		
								Standards prepared in				Standards prepared in		Percentage agreement (%)
								Extraction solvent	*E. coli* matrix			Extraction solvent	JJN-3 matrix	
NAD^+	0	0	312.5	100.5	312.5	101.8	*E. coli* 1	6963.0	6840.3	98.2	JJN-3 1	1659.5	1414.8	85.3
			2500	109.9	2500	107.6	*E. coli* 2	2391.0	2268.3	94.9	JJN-3 2	3479.8	2871.0	82.5
			7500	106.9	7500	95.3	*E. coli* 3	5606.0	5483.3	97.8	JJN-3 3	1614.5	1378.8	85.4
NADH	−64.3	−50.0	312.5	99.8	312.5	106.2	*E. coli* 1	2135.4	5197.6	243.4	JJN-3 1	909.9	1414.7	155.5
			2500	102.3	2500	117.4	*E. coli* 2	1735.8	4078.6	235.0	JJN-3 2	1344.0	2283.0	169.9
			7500	107.2	7500	102.3	*E. coli* 3	2620.4	6555.4	250.2	JJN-3 3	892.3	1379.6	154.6
$NADP^+$	0	12.5	312.5	106.3	312.5	117.6	*E. coli* 1	3211.9	3131.1	97.5	JJN-3 1	773.9	687.9	88.9
			2500	112.5	2500	118.9	*E. coli* 2	1551.4	1470.6	94.8	JJN-3 2	989.3	879.3	88.9
			7500	102.9	7500	98.4	*E. coli* 3	2325.4	2244.6	96.5	JJN-3 3	795.8	707.4	88.9
NADPH	−42.9	−1.7	312.5	108.4	312.5	118.6	*E. coli* 1	639.1	813.8	127.3	JJN-3 1	634.0	676.5	106.7
			2500	113.1	2500	115.1	*E.coli* 2	550.1	658.0	119.6	JJN-3 2	706.1	749.7	106.2
			7500	117.5	7500	107.2	*E. coli* 3	706.1	931.1	131.9	JJN-3 3	620.0	662.3	106.8
FAD^+	−3.0	−1.0	312.5	97.3	312.5	125.6	*E. coli* 1	1375.3	1629.0	118.5	JJN-3 1	832.9	846.9	101.7
			2500	112.9	2500	120.3	*E. coli* 2	945.4	1029.3	108.9	JJN-3 2	851.8	866.0	101.7
			7500	88.3	7500	114.7	*E. coli* 3	1210.7	1399.5	115.6	JJN-3 3	837.4	851.4	101.7

* Positive values denote signal enhancement and negative values indicate signal suppression.

source to acceptable purity, i.e. no response in the corresponding ^{12}C-transitions (Fig. 3). The reduced forms of NAD(P) are susceptible to oxidation and interconversion between the oxidized and reduced forms has been reported [39]. As the target metabolites and corresponding $U^{13}C$ isotopologues have identical physiochemical properties, spiking labeled internal standards into the extracts and calibration mixes at a constant ratio will allow to compensate this. Still, this approach was not considered nor mentioned in several out of the recent studies reporting pyridine dinucleotides from biological samples [4,41]. The response of flavin and pyridine nucleotides in a whole cell extract prepared from *E. coli* was recorded every hour over a 12-hour interval (Fig. 4).

Comparing A) peak area of target metabolites and B) peak area ratio of target metabolites to the area of the corresponding isotopologues, revealed that ID-correction could compensate random errors such as instrument fluctuations in a long sequence run. Matrix effects, i.e. ion signal suppression or enhancement caused by sample constituents, can also be compensated by ID, as these effects affect the target metabolites and the corresponding labeled internal standards equally, leaving the ratio unaffected. To evaluate potential matrix effects in whole cell extracts, parallelism was assessed. Parallelism describes to what extent a calibration curve prepared in solvent can be applied to reliably quantify target metabolites in biological matrices. Parallelism was evaluated by comparing the slope of a calibration curve prepared in extraction solvent to a calibration curve prepared by standard addition to whole cell extracts, and by calculating the percentage of ion suppression/enhancement. In whole cell extracts of JJN-3, no or minor signal suppression/enhancement was calculated for NAD^+, NADPH and FAD^+. A signal enhancement of 12.5 was calculated for $NADP^+$, and a signal suppression of 50.0% was calculated for NADH. In *E. coli* extracts, no or minor signal suppression/enhancement was calculated for NAD^+, $NADP^+$ and FAD^+, yet a signal suppression of 64.3, 42.9% was calculated for NADH and NADPH, respectively (Table 4). As signal suppression/enhancement for NAD^+, $NADP^+$, NADPH and FAD^+ in JJN-3, and NAD^+, $NADP^+$ and FAD^+ in *E. coli* fell within ± 15%, it was concluded that matrix effects were not significant for these metabolites. Thus, calibration curves prepared in extraction solvent could be applied for quantification. However, major signal suppression of ≥50% was calculated for both NADH and NADPH in *E. coli* extracts, and NADH in JJN-3 extracts. In order to circumvent bias from matrix effects not compensated by ID and thus allow for accurate absolute quantification of NADH and NADPH in *E. coli* extracts, and NADH in JJN-3 extract, a matched-matrix calibration approach should be applied. This reqirement is well demonstrated by the excellent agreement between quantitative results from the two sets of calibration standards for some of these compounds; being in the range of 82.5–118.5% for NAD^+, $NADP^+$, NADPH and FAD^+ in each out of three different JJN-3 extracts, and for NAD^+, $NADP^+$ and FAD^+ in three different *E. coli* extracts. And correspondingly, a poor percentage of agreement for NADH in all JJN-3 extracts (154.6–169.9%) and for NADH and NADPH in all *E. coli* extracts (119.6–250.2%) (Table 4). The latter poor percentage of agreement confirm that the matched-matrix calibration approach must be applied for absolute quantification of NADH and NADPH, and NADH in in *E. coli* and JJN-3 extracts, respectively. The suitable calibration background for each metabolite was applied to estimate the % relative recovery. In brief, the % recovery was calculated by comparing the measured concentration of three spiked samples to the pooled JJN-3 and *E. coli* extracts. The recoveries ranged from 88.3 to 125.6% for all metabolites over the three concentration ranges tested (Table 4), which is well within the acceptance criterion of ≥70%.

3.3.4. Stability

The short-term stability of the target metabolites was assessed in three QCs and biological samples under the following conditions; in auto sampler held at 6 °C for 24 h, at the bench-top for 24 h and after 1–3 repeated freeze-thaw cycles. The results are summarized in Table 5. The % recovery of all metabolites stored in autosampler at 6 °C for 24 h

Table 5
Stability of analytical standards of flavin/pyridine nucleotides quantified by the optimized LC-MS/MS method. Low, medium and high concentrations in extraction solvent (L/M/HQCs), and extracted from low, medium and high biomass (L/M/HBM) JJN-3 and *E. coli* pellets, presented under three different conditions. CV: coefficient of variation.

Compound	Sampler at 6 °C																	
	OCs						JJN-3						*E. coli*					
	LQC		MQC		HQC		LBM		MBM		HBM		LBM		MBM		HBM	
	Recovery (%)	CV %	Recovery (%)	CV %	Recovery (%)	CV %	Recovery (%)	CV %	Recovery (%)	CV %	Recovery (%)	CV %	Recovery (%)	CV %	Recovery (%)	CV %	Recovery (%)	CV %
NAD	100.4–121.2	7.8	93.1–100.3	3.1	100.4–107.2	2.8	94.9–101.3	2.7	99.6–103.8	1.6	102.3–106.0	1.5	91.9–99.4	3.0	90.7–95.9	2.3	94.7–101.7	2.8
NADH	96.4–108.5	5.3	83.9–97.2	6.4	76.5–102.8	15.6	85.8–102.7	7.0	87.3–106.3	7.6	80.0–103.5	9.4	93.1–100.2	3.2	91.6–101.9	4.2	89.0–109.0	7.5
NADP	104.5–112.3	2.9	94.2–106.1	5.1	89.6–99.4	4.7	94.9–102.3	3.0	99.6–103.8	1.6	104.1–111.8	3.0	100.8–109.8	3.7	94.3–105.6	4.7	90.7–108.2	7.6
NADPH	91.7–105.2	5.7	92.1–103.3	4.6	82.5–98.9	8.3	95.5–104.4	3.6	86.8–102.3	7.4	89.9–111.9	10.0	99.8–112.5	4.8	93.7–103.5	4.8	111.2–129.8	5.6
FAD	97.4–104.1	3.0	86.0–102.9	9.3	90.1–96.6	2.5	99.0–106.2	2.7	93.1–102.8	3.8	101.5–106.9	2.6	92.6–95.6	1.3	91.7–102.9	4.5	87.2–102.9	6.3
Bench-top (room temperature)																		
	QCs						**JJN-3**						***E. coli***					
	LQC		**MQC**		**HQC**		**LBM**		**MBM**		**HBM**		**LBM**		**MBM**		**HBM**	
	Recovery (%)	CV %	Recovery (%)	CV %	Recovery (%)	CV %	Recovery (%)	CV %	Recovery (%)	CV %	Recovery (%)	CV %	Recovery (%)	CV %	Recovery (%)	CV %	Recovery (%)	CV %
NAD	91.0–93.7	2.0	99.1–102.4	2.1	99.9–100.2	0.2	91.1–93.3	4.0	97.2–98.9	1.2	91.8–96.5	3.5	95.8–96.3	0.4	100.7–108.0	4.5	102.0–110.4	5.6
NADH	101.8–102.3	0.3	99.2–104.2	3.5	110.1–113.1	1.9	108.2–108.9	0.4	95.7–96.4	0.5	92.9–94.5	1.2	91.7–98.5	5.1	106.0–109.3	2.2	107.6–109.4	1.2
NADP	113.2–120.1	4.2	109.1–119.2	6.2	110.4–113.8	2.2	95.7–98.9	2.3	101.7–104.3	1.8	96.8–99.0	1.5	82.4–83.7	1.1	103.2–112.2	5.9	111.7–122.7	6.7
NADPH	90.6–92.0	1.1	95.9–97.4	1.0	98.7–99.2	0.4	79.8–94.0	11.5	94.6–98.0	2.5	92.5–94.4	1.5	96.7–108.5	8.1	88.8–93.7	3.8	91.5–99.7	6.1
FAD	87.7–95.1	5.7	100.0–102.9	2.1	106.4–117.4	7.0	98.1–101.0	2.0	95.3–95.7	0.3	98.8–98.5	1.2	97.2–97.4	0.2	99.9–102.6	1.9	101.6–102.6	0.7
Freeze-thaw cycles																		
	QCs						**JJN-3**						***E. coli***					
	LQC		**MQC**		**HQC**		**LBM**		**MBM**		**HBM**		**LBM**		**MBM**		**HBM**	
	Recovery (%)	CV %	Recovery (%)	CV %	Recovery (%)	CV %	Recovery (%)	CV %	Recovery (%)	CV %	Recovery (%)	CV %	Recovery (%)	CV %	Recovery (%)	CV %	Recovery (%)	CV %
NAD	98.1–107.1	4.4	92.9–104.9	6.3	98.3–102.4	2.2	91.2–94.3	1.7	97.3–101.5	2.1	97.4–99.7	1.2	95.8–96.3	0.3	98.3–106.3	3.9	100.7–102.9	1.2
NADH	99.0–106.3	3.7	96.8–103.3	3.7	101.1–107.6	3.1	105.7–108.6	1.5	97.4–100.8	1.7	92.3–96.9	2.5	96.7–99.3	1.4	101.4–105.2	1.8	99.4–104.0	2.6
NADP	104.9–120.7	7.7	103.4–106.4	1.4	103.6–108.0	2.1	92.6–97.0	2.4	101.9–104.2	1.1	96.2–98.8	1.4	73.4–75.3	1.4	92.7–100.8	4.2	103.9–109.4	2.8
NADPH	94.2–97.3	1.7	99.0–104.6	2.7	98.8–101.5	1.5	88.0–90.4	1.5	93.6–107.8	8.0	86.7–89.2	1.4	92.6–104.2	6.4	99.2–102.7	2.0	99.1–104.8	2.3
FAD	97.1–97.4	0.3	95.8–101.6	3.0	101.9–106.5	2.2	101.3–106.7	2.8	96.7–99.4	1.6	97.8–100.5	1.4	98.0–104.3	3.2	97.5–99.4	1.1	100.8–103.9	1.5

Table 6
Intracellular concentration (μM) of flavin/pyridine nucleotides in exponentially growing JJN-3 cells and *E. coli*, as quantified by the optimized extraction protocol and LC-MS/MS method. *E. coli* was cultured to OD 1.25 in mineral media.

Compound	Intracellular concentration (μM)	
	JJN-3	*E. coli*
NAD	99 ± 8	464 ± 35
NADH	51 ± 4	263 ± 40
NADP	41 ± 3	123 ± 6
NADPH	19 ± 6	28 ± 2
FAD	19 ± 1	87 ± 5

ranged from 76.5 to 129.8%. For storage on bench-top up to 24 h, the % recovery was in the range of 79.8 to 122.7%. Following freeze-thaw cycles, % recovery ranged from 73.4 to 120.7%. NAD^+, FAD^+, and NADPH were stable in the alkaline extraction solvent in all three storage conditions tested; both QCs and biological samples has maximum % loss of 9.3, 14.0, and 20.0%, respectively. These results were within the acceptable limit of stability of 20%. However, the percentage loss for NADH in HQC stored in autosampler at 6 °C for 24 h was 23.5%, exceeding that of HBM samples. Hence, NADH is seemingly more stable in biological matrix than in a pure solvent background, which might be explained by faster hydration of NADH in QC samples [23]. Stability of NADPH was good (loss < 20%) in all backgrounds, with the exception of MBM *E. coli* after 3 freeze-thaw cycles with a slightly higher loss of 26.7% loss. The lower stability upon repeated freeze-thaw might be explained by the presence of strong nucleophiles after freeze-thaw cycles, such as SO_{32-} or CN_ that can cause decomposition of both oxidized and reduced forms of pyridine nucleotides (NAD(P)H) [23]. Still the target metabolites were evaluated as stable up to 70% of the expected level at all storage conditions tested in this study, to cover the method application.

3.4. Application – Intracellular concentrations

The optimized extraction protocol and LC-MS/MS method was applied to determine the intracellular concentration of flavin and pyridine nucleotides in both biological systems described in this study, JJN-3 cells and *E. coli* (Table 6). The intracellular concentrations represent whole cell concentrations, as concentration gradients over relevant cellular compartments in the eukaryotic JJN-3 cannot be accounted for when extracting whole cells. Searching the human metabolome database (HMDB) [32] revealed that entries of the target metabolites in cell extracts were scarce. Only [NAD^+] is reported for whole cells, at a concentration of 88.7 μM, similar to the intracellular concentration in JJN-3 reported in Table 6. The ECMDB contained more relevant entries. All target metabolites but NAD^+ was reported in the μM-range, comparable to the concentrations reported herein.

4. Conclusions

A fast, robust and highly sensitive zwitterionic HILIC-MS/MS method for quantitative analysis of pyridine nucleotides from cell extracts was successfully developed and validated for low, medium and high biomass samples of two popular biological systems; *E. coli* and the human cell line JJN-3. U^{13}C-isotopologues of all target metabolites were extracted from ^{13}C-labeled *E. coli* and applied for ID, efficiently correcting random analytical variation. The method relies on zwitterionic HILIC separation resolving all target metabolites, and on positive electrospray ionization, facilitating highly sensitive detection from *E. coli* and JJN-3 cell extracts. Notably, a prerequisite for absolute quantification of NADH in JJN-3 and NADH and NADPH in *E. coli* is the preparation of calibration curves in a matched matrix. The samples are rapidly prepared without solvent removal, minimizing loss of these labile metabolites. Further, extracts were proven stable for 24 hours, allowing for long sequence runs. Altogether, this method is ideal for high-throughput analysis, and is currently employed in our laboratory to support the study of cellular phenotypes.

Funding

This work was supported by the Research Council of Norway [projects 258657 Z-fuels, 269432 AurOmega, and 248885 INBioPharm] and internal funding from NTNU (Department of Biotechnology and Food Science and Enabling Biotechnology strategic program).

CRediT authorship contribution statement

Lisa M. Røst: Formal analysis, Investigation, Methodology, Validation, Visualization, Writing - original draft, Writing - review & editing. **Armaghan Shafaei:** Formal analysis, Investigation, Methodology, Validation, Visualization, Writing - original draft, Writing - review & editing. **Katsuya Fuchino:** Formal analysis, Investigation, Methodology, Writing - review & editing. **Per Bruheim:** Writing - review & editing, Conceptualization, Funding acquisition, Supervision, Project administration.

Acknowledgements

The authors would like to thank Kåre A. Kristiansen and Susana Villa Gonzales for their technical advices and intellectual contributions to this work. The NTNU Natural Science faculty Mass Spectrometry laboratory is thanked for providing instrumentations and data processing software. The Centre for Digital Life Norway (www.ntnu.edu/dln/centre-for-digital-life-norway) is also thanked for general support of our work. The Research Council of Norway and NTNU are thanked for finacial support of this study.

Appendix A. Supplementary material

Supplementary data to this article can be found online at https://doi.org/10.1016/j.jchromb.2020.122078.

References

[1] J. Yu, J. Auwerx, Protein deacetylation by SIRT1: an emerging key post-translational modification in metabolic regulation, Pharmacol. Res. 62 (2010) 35–41.
[2] D. Holten, D. Procsal, H.L. Chang, Regulation of pentose phosphate pathway dehydrogenases by NADP+/NADPH ratios, Biochem. Biophys. Res. Commun. 68 (1976) 436–441.
[3] S.U. Bajad, W. Lu, E.H. Kimball, J. Yuan, C. Peterson, J.D. Rabinowitz, Separation and quantitation of water soluble cellular metabolites by hydrophilic interaction chromatography-tandem mass spectrometry, J. Chromatogr. A 1125 (2006) 76–88.
[4] S. Bustamante, T. Jayasena, D. Richani, R.B. Gilchrist, L.E. Wu, D.A. Sinclair, P.S. Sachdev, N. Braidy, Quantifying the cellular NAD^+ metabolome using a tandem liquid chromatography mass spectrometry approach, Metabolomics 14 (15) (2017), https://doi.org/10.1007/s11306-017-1310-z.
[5] K. Yamada, N. Hara, T. Shibata, H. Osago, M. Tsuchiya, The simultaneous measurement of nicotinamide adenine dinucleotide and related compounds by liquid chromatography/electrospray ionization tandem mass spectrometry, Anal. Biochem. 352 (2006) 282–285.
[6] C. Evans, K.L. Bogan, P. Song, C.F. Burant, R.T. Kennedy, C. Brenner, NAD^+ metabolite levels as a function of vitamins and calorie restriction: evidence for different mechanisms of longevity, BMC, Chem. Biol. 10 (2) (2010), https://doi.org/10.1186/1472-6769-10-2.
[7] X. Fu, S. Deja, B. Kucejova, J.A.G. Duarte, J.G. McDonald, S.C. Burgess, Targeted determination of tissue energy status by LC-MS/MS, Anal. Chem. 91 (2019) 5881–5887.
[8] R.M. Seifar, C. Ras, A.T. Deshmukh, K.M. Bekers, C.A. Suarez-Mendez, A.L.B. da Cruz, W.M. van Gulik, J.J. Heijnen, Quantitative analysis of intracellular coenzymes in Saccharomyces cerevisiae using ion pair reversed phase ultra high performance liquid chromatography tandem mass spectrometry, J. Chromatogr. A. 1311 (2013) 115–120.
[9] E.J.C.M. Coolen, I.C.W. Arts, E.L.R. Swennen, A. Bast, M.A.C. Stuart, P.C. Dagnelie, Simultaneous determination of adenosine triphosphate and its metabolites in human whole blood by RP-HPLC and UV-detection, J. Chromatogr. B 864 (2008) 43–51.

[10] M. Pálfi, A.S. Halász, T. Tábi, K. Magyar, É. Szökő, Application of the measurement of oxidized pyridine dinucleotides with high-performance liquid chromatography–fluorescence detection to assay the uncoupled oxidation of NADPH by neuronal nitric oxide synthase, Anal. Biochem. 326 (2004) 69–77.
[11] S. Katayama, N. Ae, R. Nagata, Synthesis of tricyclic indole-2-caboxylic acids as potent NMDA-glycine antagonists, J. Org. Chem. 66 (2001) 3474–3483.
[12] M. Kaulich, R. Qurishi, C.E. Müller, Extracellular metabolism of nucleotides in neuroblastoma × glioma NG108-15 cells determined by capillary electrophoresis, Cell. Mol. Neurobiol. 23 (2003) 349–364.
[13] M.K. Grob, K. O'Brien, J.J. Chu, D.D.Y. Chen, Optimization of cellular nucleotide extraction and sample preparation for nucleotide pool analyses using capillary electrophoresis, J. Chromatogr. B. 788 (2003) 103–111.
[14] R.M. Anderson, M. Latorre-Esteves, A.R. Neves, S. Lavu, O. Medvedik, C. Taylor, K.T. Howitz, H. Santos, D.A. Sinclair, Yeast life-span extension by calorie restriction is independent of NAD fluctuation, Science 302 (2003) 2124–2126.
[15] B. Guo, P.S. Gurel, R. Shu, H.N. Higgs, M. Pellegrini, D.F. Mierke, Monitoring ATP hydrolysis and ATPase inhibitor screening using (1)H NMR, Chem. Commun. (Camb) 50 (2014) 12037–12039.
[16] K.S. Putt, P.J. Hergenrother, An enzymatic assay for poly(ADP-ribose) polymerase-1 (PARP-1) via the chemical quantitation of NAD^+: application to the high-throughput screening of small molecules as potential inhibitors, Anal. Biochem. 326 (2004) 78–86.
[17] R. Graeff, H.C. Lee, A novel cycling assay for nicotinic acid-adenine dinucleotide phosphate with nanomolar sensitivity, Biochem. J. 367 (2002) 163–168.
[18] A. Gasser, S. Bruhn, A.H. Guse, Second messenger function of nicotinic acid adenine dinucleotide phosphate revealed by an improved enzymatic cycling assay, J. Biol. Chem. 281 (2006) 16906–16913.
[19] S. Yang, M. Sadilek, M.E. Lidstrom, Streamlined pentafluorophenylpropyl column liquid chromatography–tandem quadrupole mass spectrometry and global ^{13}C-labeled internal standards improve performance for quantitative metabolomics in bacteria, J. Chromatogr. A. 1217 (2010) 7401–7410.
[20] J. Xing, A. Apedo, A. Tymiak, N. Zhao, Liquid chromatographic analysis of nucleosides and their mono-, di- and triphosphates using porous graphitic carbon stationary phase coupled with electrospray mass spectrometry, Rapid Commun. Mass Spectrom. 18 (2004) 1599–1606.
[21] S.A. Trammell, C. Brenner, Targeted, LCMS-based metabolomics for quantitative measurement of NAD(+) metabolites, Comput. Struc. Biotec. J. 4 (e201301012) (2013), https://doi.org/10.5936/csbj.201301012.
[22] G. Zhang, A.D. Walker, Z. Lin, X. Han, M. Blatnik, R.C. Steenwyk, E.A. Groeber, Strategies for quantitation of endogenous adenine nucleotides in human plasma using novel ion-pair hydrophilic interaction chromatography coupled with tandem mass spectrometry, J. Chromatogr. A. 1325 (2014) 129–136.
[23] A. Somogyi, G. Horvai, M. Csala, B. Tóth, Analytical approaches for the quantitation of redox-active pyridine dinucleotides in biological matrices, period, Polytech Chem. Eng. 60 (2016) 218–230.
[24] F. Michopoulos, N. Whalley, G. Theodoridis, I.D. Wilson, T.P.J. Dunkley, S.E. Critchlow, Targeted profiling of polar intracellular metabolites using ion-pair-high performance liquid chromatography and -ultra high performance liquid chromatography coupled to tandem mass spectrometry: applications to serum, urine and tissue extracts, J. Chromatogr. A 1349 (2014) 60–68.
[25] E. Zborníková, Z. Knejzlík, V. Hauryliuk, L. Krásný, D. Rejman, Analysis of nucleotide pools in bacteria using HPLC-MS in HILIC mode, Talanta 205(120161) (2019) Doi: 10.1016/j.talanta.2019.120161.
[26] (a) M. Faijes, A.E. Mars, E.J. Smid, Comparison of quenching and extraction methodologies for metabolome analysis of Lactobacillus plantarum, Microb. Cell Fact. 6 (27) (2007);
(b) Samuel Aj Trammell, Charles Brenner, Targeted, LCMS-based Metabolomics for Quantitative Measurement of NAD(+) Metabolites, e201301012, Comput. Struct. Biotechnol. J. 4 (May) (2013) 27, https://doi.org/10.5936/csbj.201301012.
[27] S. Giannattasio, S. Gagliardi, M. Samaja, E. Marra, Simultaneous determination of purine nucleotides, their metabolites and β-nicotinamide adenine dinucleotide in cerebellar granule cells by ion-pair high performance liquid chromatography, Brain. Res. Protoc. 10 (2003) 168–174.
[28] J.L. Sporty, M.M. Kabir, K.W. Turteltaub, T. Ognibene, S.-J. Lin, G. Bench, Single sample extraction protocol for the quantification of NAD and NADH redox states in Saccharomyces cerevisiae, J. Sep. Sci. 31 (2008) 3202–3211.
[29] W. Zhou, S. Yang, P.G. Wang, Matrix effects and application of matrix effect factor, Bioanalysis 9 (2017) 1839–1844.
[30] U.S Pharmacopeia, Validation of compendial procedures < 1225 > , U.S.P. Convention, 2016, p. 40.
[31] O. González, M.E. Blanco, G. Iriarte, L. Bartolomé, M.I. Maguregui, R.M. Alonso, Bioanalytical chromatographic method validation according to current regulations, with a special focus on the non-well defined parameters limit of quantification, robustness and matrix effect, J. Chromatogr. A. 1353 (2014) 10–27.
[32] T. Sajed, A. Marcu, M. Ramirez, A. Pon, A.C. Guo, C. Knox, M. Wilson, J.R. Grant, Y. Djoumbou, D.S. Wishart, ECMDB 2.0: A richer resource for understanding the biochemistry of E. coli, Nucleic Acids Res. 44 (2015) D495–D501.
[33] B. Buszewski, S. Noga, Hydrophilic interaction liquid chromatography (HILIC)-a powerful separation technique, Anal. Bioanal. Chem. 402 (2012) 231–247.
[34] E. Bacalum, M. Tanase, M. Cheregi, H.Y. Aboul-Enein, V. David, Retention mechanism in zwitterionic hydrophilic interaction liquid chromatography (ZIC-HILIC) studied for highly polar compounds under different elution conditions, Rev. Roum. Chim. 61 (2016) 531–539.
[35] S. Di Palma, P.J. Boersema, A.J.R. Heck, S. Mohammed, Zwitterionic hydrophilic interaction liquid chromatography (ZIC-HILIC and ZIC-cHILIC) provide high resolution separation and increase sensitivity in proteome analysis, Anal. Chem. 83 (2011) 3440–3447.
[36] S. Kerri, M.R. Paul, Comparision of electrospray and unispray for pharmaceutical compounds, Waters technical report, Waters Corporation, Milfors, MA, USA.
[37] S. Kerri. M.A. Yun, I. Giorgis, L. Joe, W. Mark, Comparision of electrospray and impact ionization for pharmaceutical compounds, Waters technical report, Waters Corporation Mildford, MA, USA.
[38] O. Ciclet, D. Barron, S. Bajic, J.L. Veuthey, D. Guillarme, A. Grand-Guillaume Perrenoud, Natural compounds analysis using liquid and supercritical fluid chromatography hyphenated to mass spectrometry: evaluation of a new design of atmospheric pressure ionization source, J. Chromatogr. B. 1083 (2018) 1–11.
[39] W. Lu, L. Wang, L. Chen, S. Hui, J.D. Rabinowitz, Extraction and quantitation of nicotinamide adenine dinucleotide redox cofactors, Antioxidants & Redox Signal. 28 (2017) 167–179.
[40] K. Ortmayr, J. Nocon, B. Gasser, D. Mattanovich, S. Hann, G. Koellensperger, Sample preparation workflow for the liquid chromatography tandem mass spectrometry based analysis of nicotinamide adenine dinucleotide phosphate cofactors in yeast, J. Sep. Sci. 37 (2014) 2185–2191.
[41] K. Yaku, K. Okabe, T. Nakagawa, Simultaneous measurement of NAD metabolome in aged mice tissue using liquid chromatography tandem-mass spectrometry, Biomed. Chromatogr. 32 (6) (2018), https://doi.org/10.1002/bmc.4205.